



**HAL**  
open science

## Experimental and numerical investigations on wide fuselage configurations for a business jet aircraft

Guillaume Arnoult, Aristeidis Antonakis, Olivier Atinault, Alberto Baretter, Jérôme Delva, Michaël Meheut, Vianney Nowinski, Clément Toussaint

### ► To cite this version:

Guillaume Arnoult, Aristeidis Antonakis, Olivier Atinault, Alberto Baretter, Jérôme Delva, et al.. Experimental and numerical investigations on wide fuselage configurations for a business jet aircraft. EUCASS-CEAS 2023, EUCASS, Jul 2023, Lausanne, Switzerland. 10.13009/EUCASS2023-543 . hal-04265292

**HAL Id: hal-04265292**

**<https://hal.science/hal-04265292v1>**

Submitted on 30 Oct 2023

**HAL** is a multi-disciplinary open access archive for the deposit and dissemination of scientific research documents, whether they are published or not. The documents may come from teaching and research institutions in France or abroad, or from public or private research centers.

L'archive ouverte pluridisciplinaire **HAL**, est destinée au dépôt et à la diffusion de documents scientifiques de niveau recherche, publiés ou non, émanant des établissements d'enseignement et de recherche français ou étrangers, des laboratoires publics ou privés.



Distributed under a Creative Commons Attribution - NonCommercial 4.0 International License

# Experimental and Numerical Investigations on Wide Fuselage configurations for a Business Jet aircraft

Guillaume ARNOULT<sup>1\*</sup>, Aristeidis ANTONAKIS<sup>2</sup>, Olivier ATINAULT<sup>1</sup>, Alberto BARETTER<sup>3</sup>, Jérôme DELVA<sup>3</sup>,  
Michaël MEHEUT<sup>1</sup>, Vianney NOWINSKI<sup>3</sup>, Clément TOUSSAINT<sup>2</sup>

<sup>1</sup> ONERA, 8 Rue des Vertugadins, 92190 MEUDON, France

<sup>2</sup> ONERA, 2 Avenue Edouard Belin, 31000 TOULOUSE, France

<sup>3</sup> ONERA, 5 Rue des Fortifications, 59045 LILLE, France

[guillaume.arnoult@onera.fr](mailto:guillaume.arnoult@onera.fr), [aristeidis.antonakis@onera.fr](mailto:aristeidis.antonakis@onera.fr)

<sup>†</sup> Corresponding Author

## Abstract

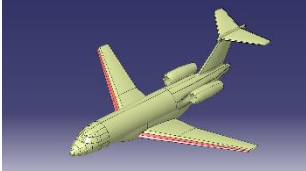
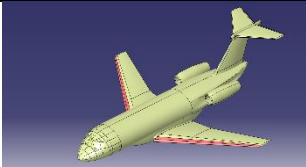
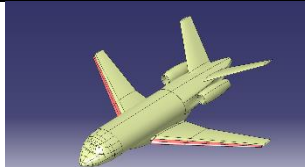
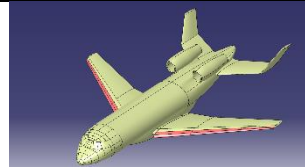
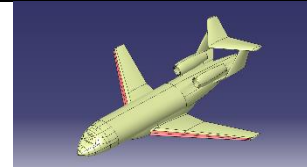
The wide fuselage configuration is regarded as one of the most promising candidates for improving the fuel efficiency of business jet aircraft by increasing the cabin internal volume. In this article, several such configurations are investigated both numerically and experimentally to evaluate the impact of fuselage shape on aerodynamic performance and stability, including a wind tunnel test campaign at the ONERA L1 Lille wind tunnel. An analysis of the results is presented, comprising a parametric study on the interaction between fuselage width and tail configuration. Finally, an improved tail sizing process is proposed for the new configurations addressing the limitations of existing approaches.

## 1. Background

The fuel consumption reduction is one of the major challenges for the design of new aircraft. One way to attain this objective consists in increasing the width of the fuselage and thus its internal volume, leading to an overall reduction of the fuel consumption per square meter of cabin space. The concept of a wide fuselage has previously been studied by Drela [1] through the development of the D8 aircraft concept and by Wiart et al. [2] with the additional aim of integrating the engines into the fuselage.

In the scope of the European Clean Sky 2 (ITD Airframe), ONERA and DLR investigated several unconventional aircraft solutions that could significantly reduce the environmental impact of air transportation in the near future for SMR (Small-Medium Range) and business jet missions. For this second mission, the wide-fuselage configuration (referred as LF hereafter) is one of the most promising concepts. In the frame of the project, several tail shapes were selected to equip this configuration with a view to exploring the design space and identifying the associated performance tradeoffs. An illustration of the tested configurations is presented in Table 1; derivatives with varying engine positions were also added during the campaign.

As described above, the overall objective of this study was the evaluation and comparison of several tail design and fuselage width configurations for business jets from a stability and performance standpoint. To this end, variable-fidelity tools were used during the process to size or validate the potential of each design. In the following paragraphs, a description of the overall methodology is given, followed by details on the element sizing and model manufacturing procedures.

T-Tail	V-Tail	U-Tail	Pi-Tail
 Cylindrical fuselage			
			

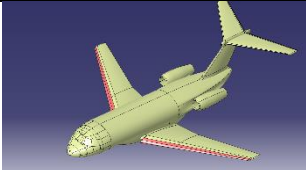
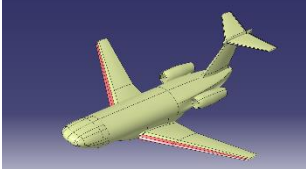
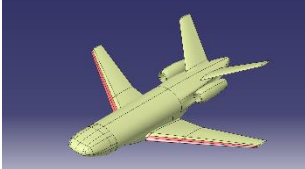
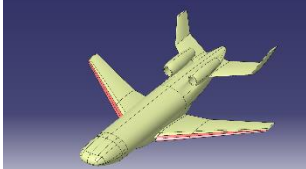
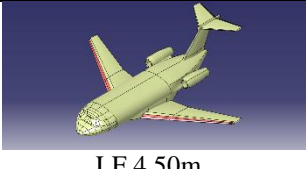
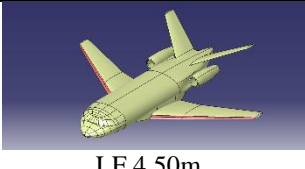
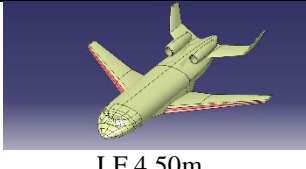

LF 3,50m	LF 3,50m	LF 3,50m	LF 3,50m
 LF 3.50m variation 15m <sup>2</sup>			
 LF 3.50m with NOVA nose	 LF 3.50m with NOVA nose	 LF 3.50m with NOVA nose	
 LF 4.50m	 LF 4.50m	 LF 4.50m	 LF 4.50m

Table 1 - Summary of the models tested during the wind tunnel campaign (LF: Large Fuselage).

## 2. Description of the Wind Tunnel models sizing

### a. Preliminary sizing procedure of the tail shapes

Prior to the wind tunnel test campaign, the surface sizing of each tail shape selected was performed, based on Handling Qualities (HQ) analyses, to ensure that the tested configurations possess suitable characteristics from a stability and control standpoint. The objective of this sizing step lies in the identification of the minimum surface of the tail planes ensuring a given, qualitative or quantitative, level of HQ based on a series of criteria set by the designer. In this study, the evaluation of the latter was based on an in-house tool developed at ONERA, combined with the AVL solver [3] for aerodynamic modelling. This sizing module returns the range of center of gravity (CG) positions satisfying the set longitudinal and lateral HQ criteria as function of tail size: Following this, the minimum tail surface corresponding to the desired CG range is selected. Indicative results of this optimization process are presented in Figure 1 for the horizontal tail plane (HTP) surfaces.

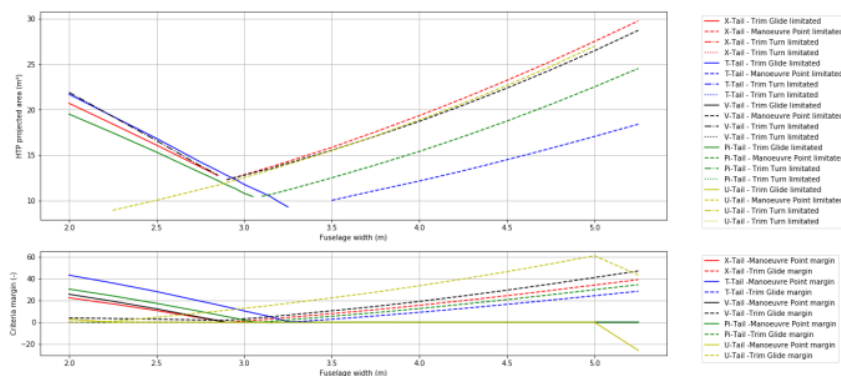


Figure 1 - Optimization results on HTP. Above: HTP area w.r.t. fuselage width, the lower the better. Below: Criteria margin (only sizing criteria are displayed)

As a general conclusion from this preliminary analysis, the tails of configurations with narrower fuselage profiles were sized by a trim-at-glide condition, a control-authority or forward-CG criterion, while the ones with wider fuselage were sized by the maneuver point location, a stability-related condition, the fuselage aerodynamic effect increasing with increasing width. Thus, two main trends were identified, associated to the fuselage aerodynamic center's forward location:

- The aircraft neutral point, related to its maneuver point, moves forward, therefore for the same CG position, the aircraft will be less stable in the longitudinal axis.
- The reduced longitudinal stability reduces the pitch control deflections required for trimming and maneuvering the aircraft, leading to increased forward-CG range.

For the wind tunnel test campaign, the sizing results obtained for the 3.50 m-wide fuselage were selected for the manufacturing of the tail shapes.

### b. Wind tunnel conditions

The main objective of the wind tunnel test campaign was to evaluate the static and dynamic aerodynamic coefficients (including their dynamic derivatives). To this end, the test campaign was performed in the ONERA L1 wind tunnel using the PQR device illustrated in Figure 2 with the reference configuration installed. This allows for performing static and dynamic measurements while the model is rotated around its axis.



**Figure 2 - Illustration of the PQR device used during the NACOR LF Wind Tunnel test campaign**

The general wind tunnel flow conditions are presented in Table 2, with the Reynolds number being based on the Mean Aerodynamic Chord (MAC) of the model.

Open L1 test section		
Flow Velocity (m/s)	35	60
Mach number	0.103	0.176
Pressure (Pa)	101 325	
Temperature (K)	288	
Reynolds number based on the model MAC	361 207	617 209
Angle of attack range (°)	[-15 ; 25]	
Angle of sideslip range (°)	[-20 ; 20]	

**Table 2 - Measurements conditions inside the wind tunnel**

All model variants were equipped with transitional devices (ZigZag tapes) on the wing and the fuselage located at 5 % and 15 % of the chord length. The positions of these devices were determined through 2D elsA [4] RANS computations of the wing profiles and of the fuselage.

### c. Manufacturing of the models for the Wind tunnel

#### Conception of modular models

In total, seventeen (17) configurations were selected for testing, comprising a combination of the fuselage widths, tail shapes and engine positions, with common parts for most of the models (e.g. nose or tails). During the design and manufacturing phases, a modular approach was adopted: All the configurations were assembled using a common internal mechanical interface illustrated in Figure 3.

The 6-component balance, used to measure the global forces (lift, sideforce and drag) and the moments (rolling, pitching and yawing) acting on the models, was placed inside this common interface, to which the fuselage parts and the wings were fixed. In the case of the wide-fuselage configurations, a dedicated interface was designed, which allowed for shifting the wing root chord in the spanwise direction. This middle part of the aircraft was then completed by adding the various front and rear elements to reproduce the forms of the tested configurations with a limited number of reconfiguration steps. The four tail shapes are illustrated in Figure 3, for the 3.5m-wide fuselage, also showcasing the interchangeable model elements required for switching from one configuration to the other.



**Figure 3 - Modifications of the model to switch from one configuration to the others, illustrated for LF 3.50 m**

As can be observed in the Figure 3, a simple replacement of the upper rear-part of the T-Tail configuration was required to obtain the V-Tail configuration, while the changes required to switch from the V-Tail configuration to the Pi- or U-Tail configurations necessitated a complete modification of the rear part of the fuselage.

### 3. Numerical study of the aircraft configurations

#### Definition of the CFD mesh

The Pointwise meshing software was employed to create CFD meshes for a number of selected configurations, with simulations being run for angles of attack in the range  $\alpha \in [-10 ; 25]^\circ$  and sideslip angles  $\beta \in [0 ; 10]^\circ$ . Compared to the experimental test matrix, the number of configurations was reduced, the study's main focus being on the validation of the CFD models' ability to capture the trends of the aerodynamic coefficient with angle of attack and sideslip.

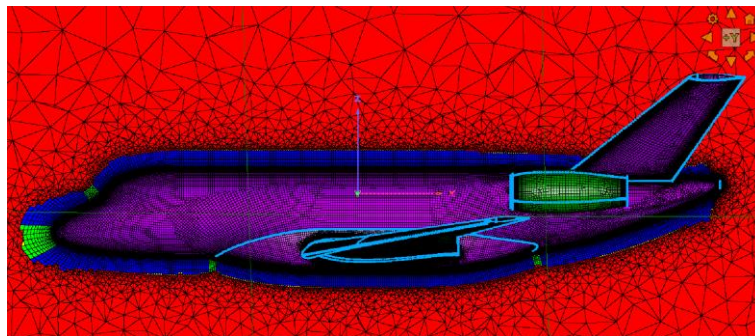


**Figure 4 - Illustration of the RANS mesh generated with Pointwise**

The boundary layer developing over the skin of the aircraft was discretized with 51 cells: The size of the first cell was fixed at  $h = 5 \cdot 10^{-6} m$  to ensure a  $y^+ < 1$  for the CFD computations and the growth rate between two consecutive cells was set at 1.15.

#### CFD solver parameters

The CFD computations were performed using the SU2 software [5] considering a RANS modelling of the flow, combined with the Spalart-Allmaras turbulence model. The Mach number considered for these computations was  $M = 0.2$  at the atmospheric conditions of the wind tunnel.

The reference surface and length used for the extraction of the aerodynamic force and moment coefficients were the surface of the wing planform ( $S_{ref} = 0,13 m^2$ ) and Mean Aerodynamic Chord (MAC -  $L_{ref} = 0,15 m$ ) respectively. Finally, the reference point considered for the computation of the moments was defined at  $(x, y, z)_{ref} = (0.52, 0, -0.07) m$  from the aircraft nose, corresponds to the 25% MAC location.

## 4. Comparison between experimental and numerical measurements

### Influence of the fuselage shape

This Section is aimed at presenting an overview of the effects of fuselage geometry on the aircraft aerodynamic coefficients: Under this scope, the configurations of Table 1 are hereby compared to the reference cylindrical aircraft configuration.

Measurements of the complete aerodynamic tensor, also including the results of the respective CFD calculation of the coefficients, are presented in Figure 5 for the reference and the LF 3.50 m configurations: Each configuration is associated to a color, while in Figure 5.a the lift coefficient curves are represented by solid lines and drag coefficient curves are associated to the dashed lines. Finally, the results of the CFD computations are represented by dots, maintaining the same color code for the different configurations as for the measurements.

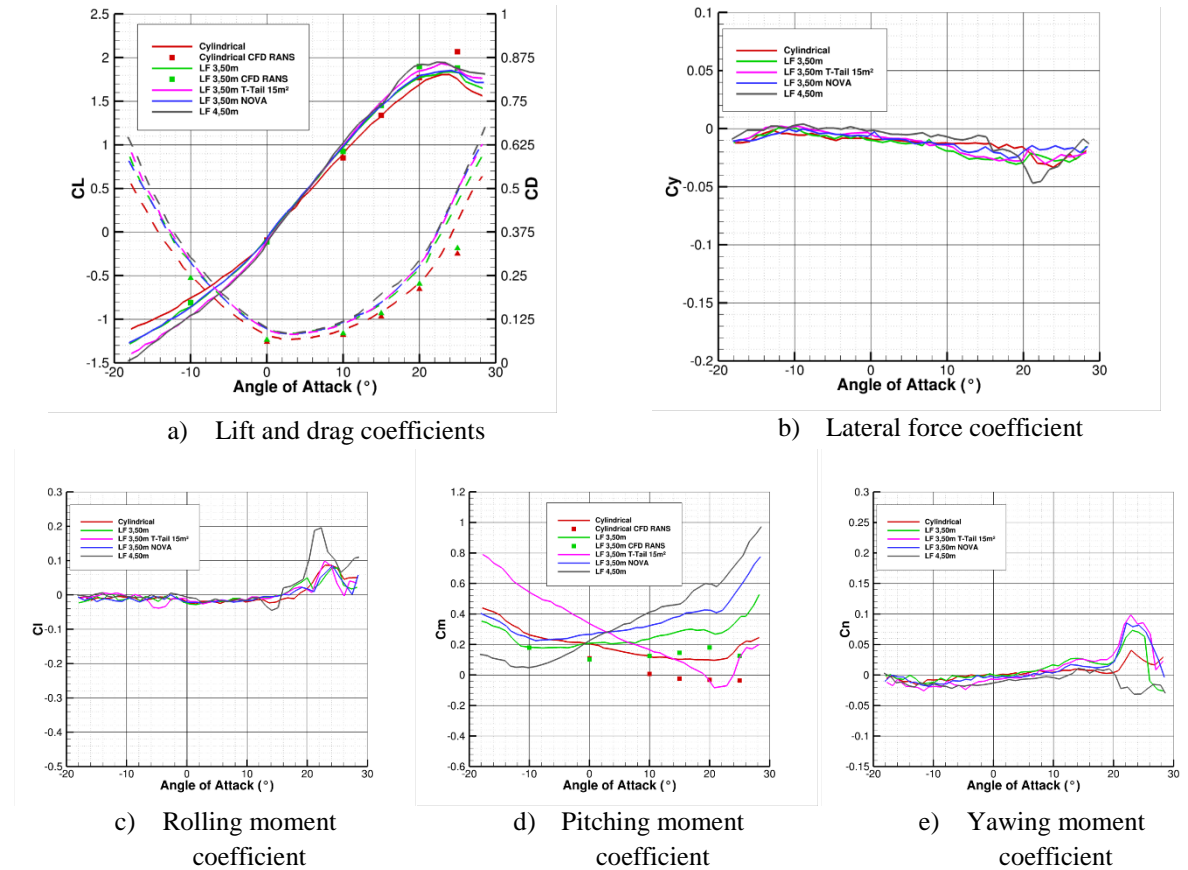


Figure 5 - Comparison of the aerodynamic coefficients at  $\beta = 0^\circ$

At a first sight, it appears that the increase of the fuselage width tends to increase the drag measured compared to the reference (dashed red line in figure Figure 5.a) while the effect on the lift coefficients is quite limited even if the gradient of lift  $\frac{dC_L}{d\alpha}$  tends to increase slightly with the increase of the fuselage width.

As far the drag increase effect is concerned, this was found to be driven by two main contributions: Firstly, the increase in fuselage width leads to an increase of the friction drag in a manner proportional to the wetted surface. Secondly, when the 3.50 m or 4.50 m models were installed in the wind tunnel, the wing root section was moved toward the spanwise direction, leading to an increase of the wingspan and thus to a reduction of the theoretical induced drag.

As far as longitudinal stability is concerned, the tailplanes selected for the manufacturing and testing were pre-sized for the fuselage width of 3.50 m: This configuration (green curve in Figure 6) was thus expected to be stable, which was only marginally the case in experimental and CFD results. Therefore, the neutral point for these configurations is located close to the measurement reference point. The configuration equipped with the NOVA nose cone showcases the same longitudinal static stability as the LF 3.50 m configuration, the only difference being the value of the zero-lift pitching moment  $Cm_0$ , which was by-design more positive for the NOVA configuration. The additional T-Tail

geometry with an increased horizontal surface of 15 m<sup>2</sup> (equal to that of the reference LSBJ configuration) was shown to be the most stable among the tested configurations, denoted by a more pronounced negative gradient  $\frac{dC_m}{d\alpha} < 0$ . Finally, increasing fuselage width to 4.50 m leads to longitudinal instability for all tested configurations.

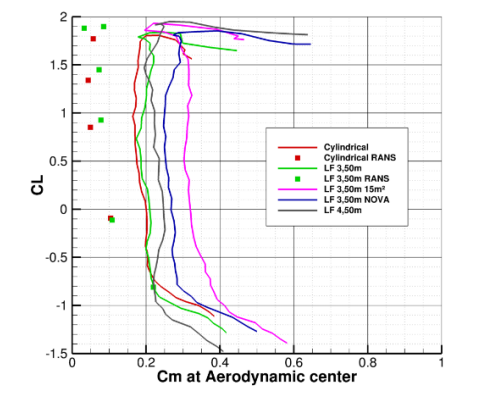


Figure 6 - Influence of the fuselage width on the position of the aerodynamic center

### Influence of the tail shape

The influence of the tail type on the aerodynamic measurements was investigated for a fuselage width of 3.50 m on the configurations presented in Table 1. Under this scope, CFD RANS computations were performed for all of these configurations except for the Pi-tail. In addition, estimations of the coefficients obtained from the VLM approach used during the sizing process were compared to the experimental measurements and CFD evaluations.

The variations of the aerodynamic coefficients for these configurations are presented in Figure 7 as function of angle of attack: experimental measurements are represented by solid lines, the CFD results by squares and the VLM results in by dashed lines and circular markers. Since the AVL calculation is based on potential flow theory, the associated drag coefficient predictions are not presented in Figure 7.c.

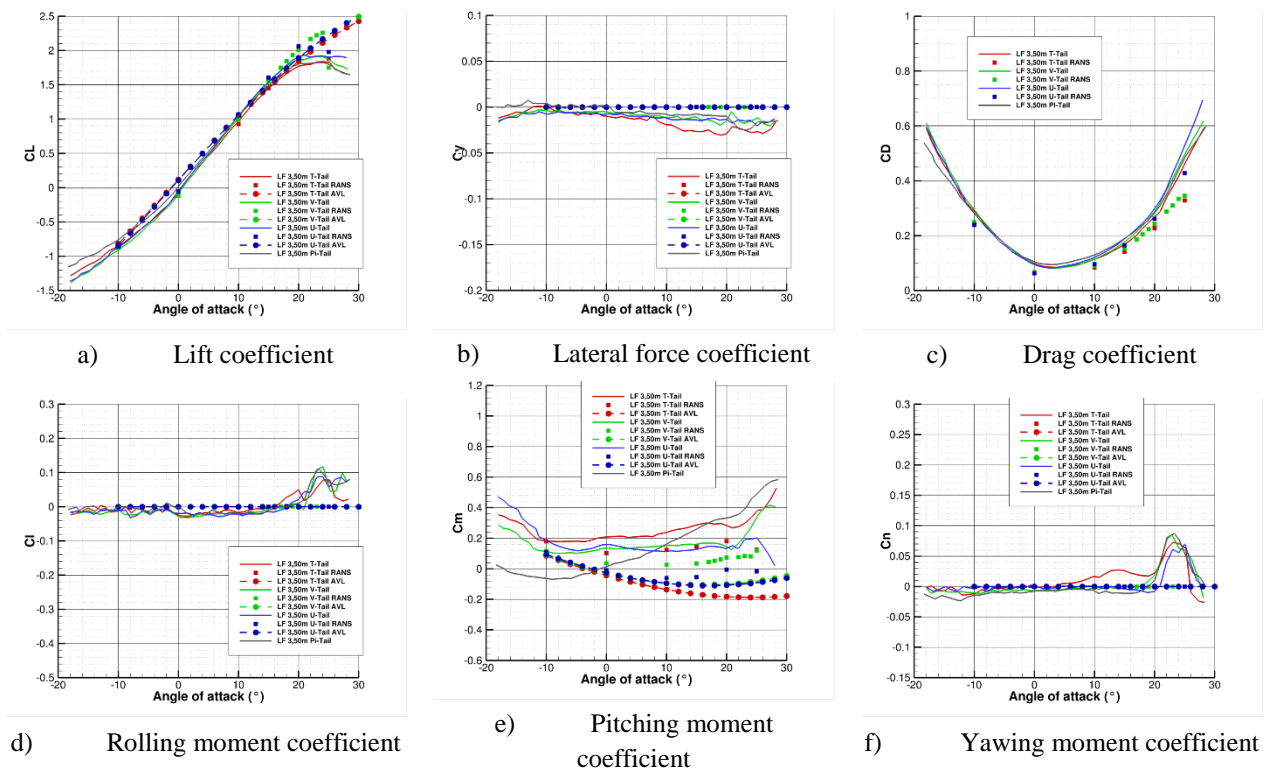
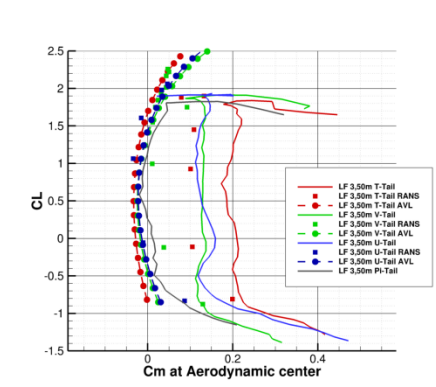


Figure 7 - Influence of the Tail shape on the polar evolution of the aerodynamic coefficients,  $\beta = 0^\circ$

The presented results indicate that the lift coefficients were generally well approximated by the CFD simulations and the VLM method in their linear regime ( $-5^\circ \leq \alpha \leq 20^\circ$ ). The stall appears at a slightly higher angle of attack in the RANS computations compared to the wind tunnel measurements, as illustrated for the LF 3.50m V-Tail configuration (green squares) in Figure 7.a.

The evolution of the pitching moment coefficient predicted by the VLM method (in Figure 7.e) was, however, not in good agreement with experimental data. As a result, the gradients modeled by the VLM decrease for  $-10^\circ \leq \alpha \leq 15^\circ$  (up to  $21^\circ$  for the T-Tail), suggesting that the configurations should be statically stable in the longitudinal axis, contrary to what was observed in the wind tunnel results. These conclusions were nevertheless in agreement with the CFD estimation of the pitching moment coefficient except for a difference in  $Cm_0$ , as was already observed during the study of the influence of the fuselage width. Figure 8 presents an overview of the results obtained on longitudinal static stability.



**Figure 8 - Influence of the tail shape on the position of the aerodynamic center**

Considering these variations of the aerodynamic coefficients, it appears that some adjustments of the VLM approach are needed before considering it is completely relevant for the pre-sizing of the tail areas and shapes: This is part of the complementary analysis included in the following Section and applied to the re-sizing of the V-Tail configuration using a combination of experimental and variable-fidelity numerical data.

## 5. Stability and Control Effects Analysis

Following the completion of the wind tunnel test campaign, a new iteration of the aerodynamic model identification process was performed in order to assess the accuracy of the models used for preliminary design and to provide improved estimates for re-sizing the tested configurations. Due to the large volume of data, a set of polynomial models were fitted to the experimental results, to facilitate comparisons between the different configurations. A parametric analysis was performed in order to identify the aerodynamic phenomena related to specific configuration characteristics and assess their effects on aircraft stability and control.

### Fuselage width aerodynamic effect (Tail-OFF)

A comparison of results corresponding to the tailless configurations of the ‘nominal’ fuselage shape (Figure 9 and Figure 10) led to the following conclusions:

- As expected, increased fuselage width leads to increased drag coefficient ( $C_x$ ), however, the drag penalty appears to be smaller in magnitude than the associated increase in internal volume. This finding confirms that the cabin-volume-to-drag ratio is improved for wider fuselage cross sections.
- Wider fuselage cross-sections increase the slope of the lift coefficient ( $C_z$ ) with angle of attack, as a result of the increase in horizontal projected area. However, the zero-lift angle of attack of the wing-fuselage configuration is also affected, causing a reduction in  $C_z$  at low angles of attack.
- Due to the increased lift generated by a wider fuselage, a strong destabilization of the longitudinal (pitch) axis occurs due to a forward shift of the neutral point of the wing-fuselage configuration.
- Being ‘slenderer’ and more ‘streamlined’ about the lateral axis, a wider fuselage profile reduces side force due to sideslip ( $C_{y\beta}$ ) and, consequently, the instability in the directional (yaw) axis. Similar effects are also visible in the roll axis, probably due to the effect of fuselage profile on the crossflow under sideslip; their nature, however, is non-linear and additional data would be required to reach a safe conclusion.



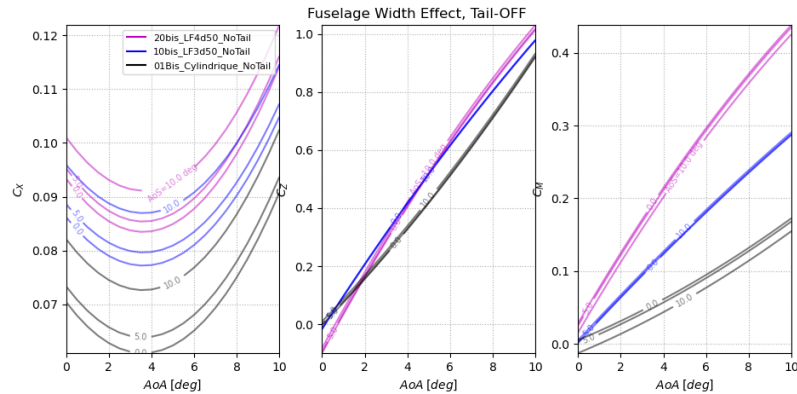


**Figure 9 - Fuselage width effect on longitudinal aerodynamic coefficients: Comparison of Tail-OFF results for the 2.5 m cylindrical fuselage [black], 3.5 m [blue] and 4.5 m [magenta] elliptical profiles.**

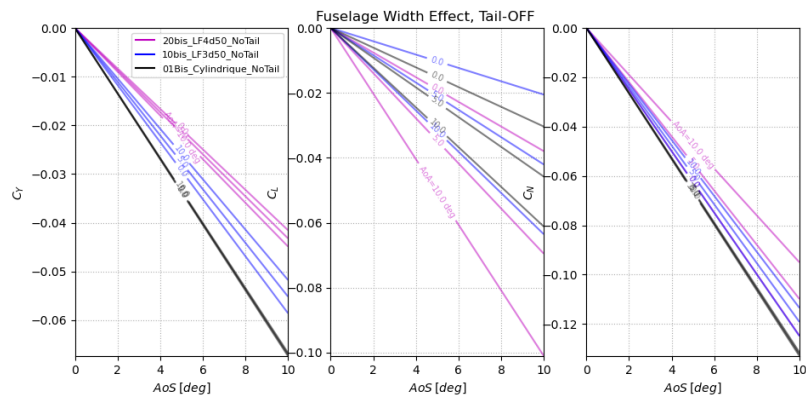


**Figure 10 - Fuselage width effect on lateral/directional aerodynamic coefficients: Comparison of Tail-OFF results for the 2.5 m cylindrical fuselage [black], 3.5 m [blue] and 4.5 m [magenta] elliptical profiles.**

### Tail Configuration Comparison

By subtracting predictions for Tail-OFF configurations from the associated results for the Tail-ON cases, the empennage aerodynamic effects could be isolated and studied:  $[Tail\ effect] = [Tail\ ON] - [Tail\ OFF]$ . A summary of the results obtained is presented in Figure 11 and Figure 12 for a 3.5 m-wide fuselage. Based on the latter, it may be concluded that:

- As far as directional stability is concerned, the U, V and Pi tail configurations appear to be largely undersized compared to the T-tail case.
- The rolling moment of the U and V tail configurations shows a strong dependency to the angle of attack.
- The T and V tails offer better stabilization in pitch for a given drag penalty than the U tail. If the combined effects on longitudinal and lateral stability are equally considered, the T-tail offers the best overall performance; this is combined with the highest  $C_{m0}$  value, which should also have a secondary positive effect on trim drag.
- The Pi-tail appears to suffer from an interference effect with its pitch stabilization effect being significantly lower than that of the other configurations, despite having the highest overall drag contribution.

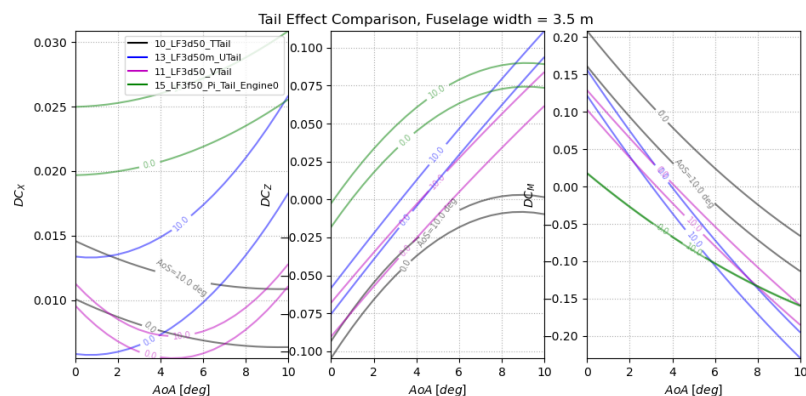


**Figure 11 - Longitudinal aerodynamic coefficients for T-tail [black], U-tail [blue], V-tail [magenta] and Pi-tail [green] configurations.**

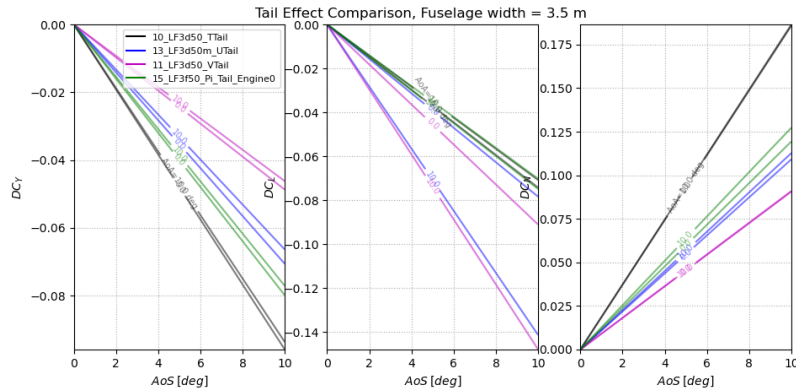


Figure 12 - Lateral/directional aerodynamic coefficients for T-tail [black], U-tail [blue], V-tail [magenta] and Pi-tail [green] configurations.

### Fuselage Width Effect on Tail Effectiveness

In order to evaluate how each tail configuration interacts with high-width fuselage shapes, a dedicated analysis was performed comparing the extracted tail effects for 3.5 and 4.5 m-wide fuselage cross sections. The effects of increased fuselage width are summarized in Table 3 and Figure 13 to Figure 17 for each tail configuration.

Tail Configuration	Fuselage width Effect				
	$DC_x$	$DC_z$	$DC_{m_a}$	$DC_{m_0}$	$DC_{n_b}$
T	Negligible	Negligible	Small reduction	Negligible	Reduced
U		Small increase	Reduced	Reduced	
V	Increased	Small variation	Small reduction	Negligible	Small reduction
Pi			Strong reduction	Reduced	

Table 3 - Summary of the effects of increased fuselage width on the aerodynamic coefficients of each tail configuration.

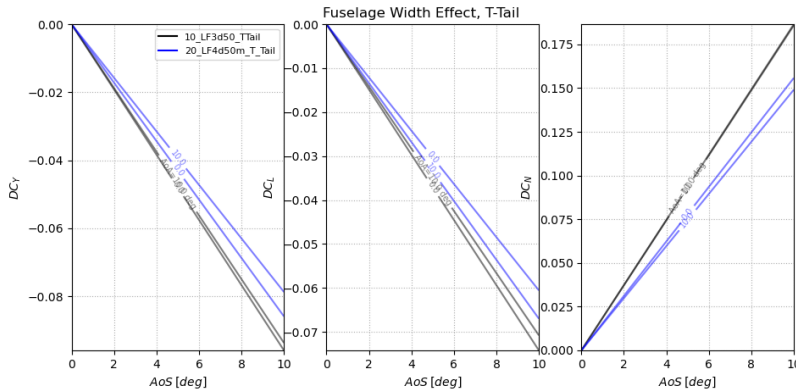


Figure 13 - Comparison of lateral/directional aerodynamic coefficients for the T-tail configuration for fuselage widths of 3.5 m [black] and 4.5 m [blue].

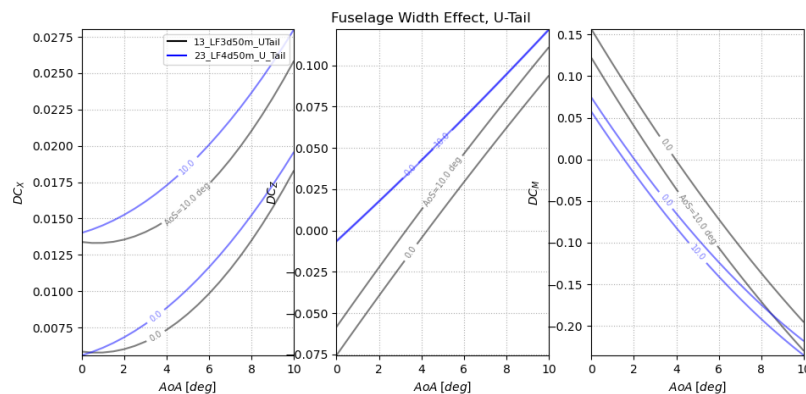
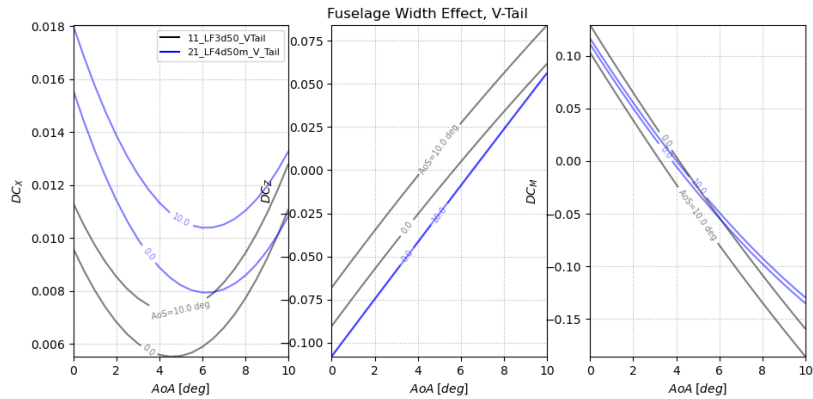
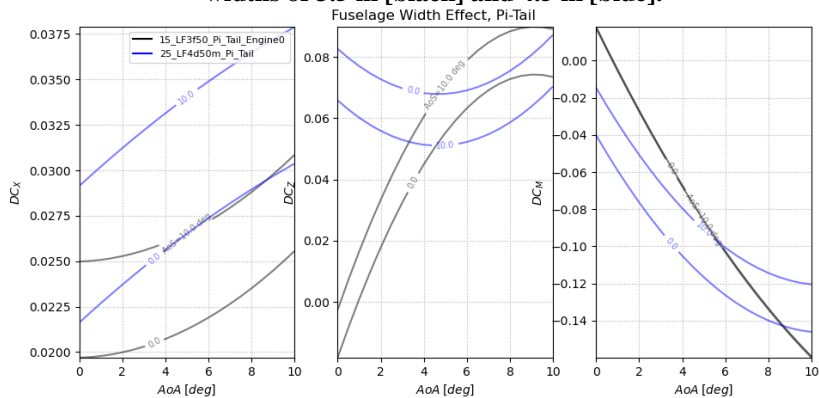


Figure 14 - Comparison of longitudinal aerodynamic coefficients for the U-tail configuration for fuselage widths of 3.5 m [black] and 4.5 m [blue].



**Figure 15 - Comparison of longitudinal aerodynamic coefficients for the V-tail configuration for fuselage widths of 3.5 m [black] and 4.5 m [blue].**



**Figure 16 - Comparison of longitudinal aerodynamic coefficients for the Pi-tail configuration for fuselage widths of 3.5 m [black] and 4.5 m [blue].**

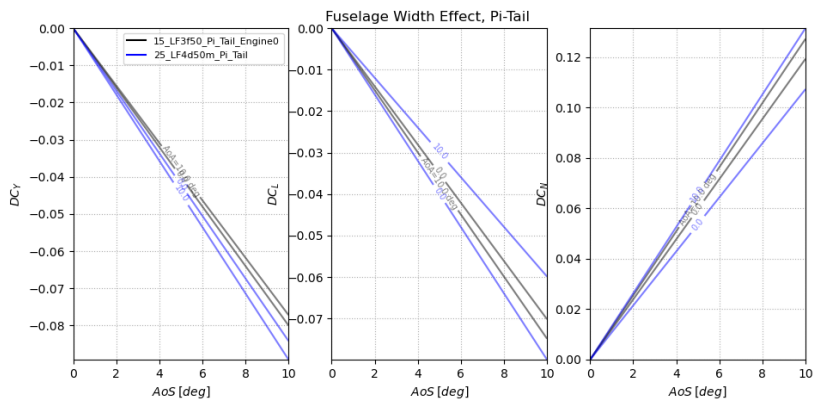


**Figure 17 - Comparison of lateral/directional aerodynamic coefficients for the Pi-tail configuration for fuselage widths of 3.5 m [black] and 4.5 m [blue].**

## 6. Enhancement of tail sizing capabilities

### Limitations of low-fidelity preliminary sizing methods

In the majority of the tested configurations, an analysis of WT data unveiled unstable characteristics in the longitudinal and directional axes. Using the WT results, a preliminary calculation of correction factors for tail sizing was performed where tail sizes of all wide-fuselage configurations were updated in order to reproduce the longitudinal and lateral static stability margins of the reference configuration. The outcome of this analysis indicated that, in many cases (especially for the 4.5m-fuselage-width configurations), the re-calculated tail surface was more than 50% larger than that estimated during initial sizing (Figure 18)

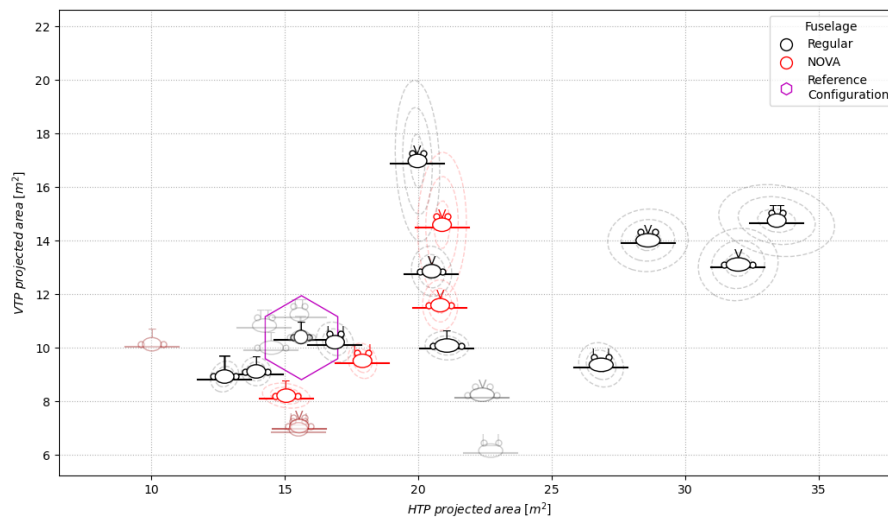


**Figure 18 - HTP / VTP projected area of tested configurations: Initial sizing results (semi-transparent symbols) VS re-calculated sizing using WT data (solid-line symbols). Dashed contours represent iso-covariance error ellipses.**

An investigation of the discrepancy between AVL and the experimental data was conducted in order to identify its root cause. The analysis performed was based upon a comparison of the VLM model output to that of the WT-data-trained polynomial models, isolating, where applicable, the effects of individual airframe components. The main error sources were identified as:

- Incorrect representation of the fuselage aerodynamic effect;
- Numerical effects, leading to incorrect modelling of the inter-component aerodynamic interaction: in the absence of reference data (e.g. WT results) the latter may be difficult to distinguish from ‘real’ aerodynamic effects.

Under this scope, the predictions of an in-house VLM code were also compared to the reference data, and were shown to be more accurate than the initial AVL results due to the improved handling of numerical effects. Despite this, the investigation highlighted a key limitation of VLM approaches when the modelling of ‘thick’ bodies is required: there exists little theoretical justification for the usual ‘cross’-type representation of fuselage and nacelle geometries and, in case of geometries with considerable thickness-to-length ratios, VLM predictions do not match experimental results sufficiently well. More sophisticated low-fidelity aerodynamic modelling techniques, including combinations of different elements (e.g. vortices, doublets, sources/sinks) do exist, however, the added complexity is not justified by the resulting improvement in modelling accuracy.

### Multi-fidelity sizing process

Despite the previously-discussed limitations of the low-fidelity aerodynamic solutions, the latter remain a useful tool for the preliminary analysis of aircraft configurations because they allow for rapid prototyping during a phase where the detailed aircraft geometry is largely undefined. On the other hand, one needs to address the issues related to modelling precision if useful conclusions are to be extracted from the aerodynamic analysis. This may be achieved by effectively combining predictions with higher fidelity results, once these become available.

In this regard, despite their limited overall accuracy, the ability of lower-fidelity methods to estimate trends or ‘gradients’ around a reference point may be exploited: Using high-fidelity data to provide a reference, a low-fidelity aerodynamic solver may be used to estimate increments associated to variations in the configuration characteristics (e.g. tail surface area, chord etc). As a result, by exploiting higher fidelity results, the variance of the combined predictions is reduced compared to the simple low-fidelity case.

Extending the concept even further, an ‘optimized’ sizing process can be elaborated as a series of embedded variable-fidelity sizing loops, leading to improved accuracy and less development cost / risk. An example schematic representation of this process, applied to the case of tail surface sizing, is depicted in Figure 19.

The proposed process begins with a set of reference aerodynamic data, which can be of any type, depending on the state of aircraft development. A low-fidelity solver (e.g. VLM), coupled with a handling qualities analysis tool is employed to calculate tail surface increments which are used to modify a higher-fidelity model (in this example, a RANS solver) whose results provide an update for the reference data, also in the form of an aerodynamic increment. The above process is repeated until the output of successive iterations become sufficiently similar with respect to an empirically (or statistically) defined convergence threshold  $\epsilon_1$ . Finally, in a similar manner, a second condition can be

applied to the output of the internal sizing loop to decide whether an additional WT evaluation is required in order to update the reference data, based upon a second threshold  $\varepsilon_2$ . The sizing loop process is terminated when its output is sufficiently close to the reference data.

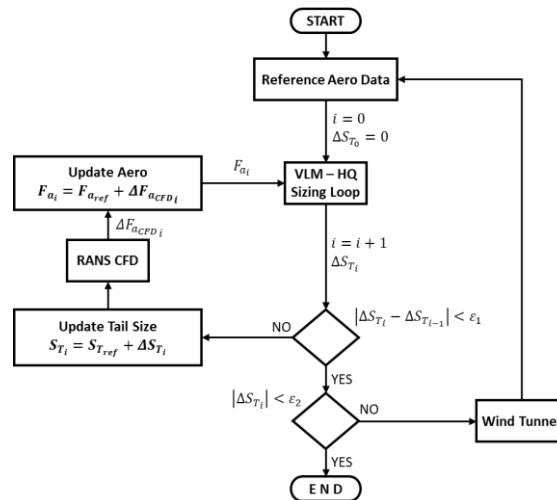


Figure 19 - Flowchart of the proposed multi-fidelity process for aircraft tail sizing

### Case Study: V-Tail sizing

#### Low-Fidelity re-sizing

A test application on the sizing of the 3.5 m fuselage V-tail configuration was selected to demonstrate the concept of the proposed multi-fidelity sizing process, using the available WT results as the initial reference data. The in-house MVS VLM solver was employed to provide low-fidelity aerodynamic results in conjunction with the SU2 RANS solver which was used as a medium-fidelity model to complete the design loop.

Using the WT model geometry as reference, the MVS solver was used to calculate sensitivities of the aerodynamic parameters with respect to scale factors applied to the horizontal and vertical empennage projected areas. The resulting ‘incremental’ aerodynamic derivatives are shown in Figure 20, as function of the horizontal (Ksh) and vertical (Ksv) scale factors. Interestingly, due to nature of the V-tail configuration, the diagonal orientation of most contours of the same Figure suggests that there exists a non-negligible interaction between the two axes from an aerodynamic perspective. Finally, an interpolation scheme was employed to generate surrogate models for each aerodynamic effect, which were subsequently combined with a Handling Qualities sizing process to estimate the required scaling for the empennage horizontal and vertical projected areas.

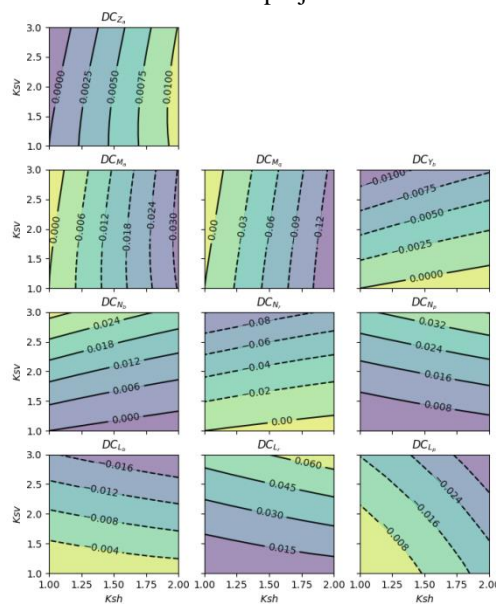


Figure 20 - Aerodynamic derivative increments as function of horizontal (Ksh) and vertical (Ksv) empennage scale factor.

Longitudinal and lateral/directional sizing were performed separately, based on the ‘classic’ decoupled-axis assumption. However, as previously pointed out, this does not totally hold for the case of the selected V-tail configuration. As a result, an iterative approach, comprising sequential longitudinal and lateral/directional sizing calculations, was necessary to obtain converged values for the horizontal and vertical tail scale factors.

Figure 21 and Figure 22 present the results of the HQ sizing process for the longitudinal and lateral/directional cases respectively. A CG range of 30% Mean Aerodynamic Chord (MAC) was set as the target for the tail re-sizing. The longitudinal sizing was defined by the Flare and Neutral Point conditions (Figure 21) whereas the lateral one was driven by the VMC requirement (Figure 22). The resulting scale factors were 1.32 and 1.97 for the horizontal and vertical tail area respectively.

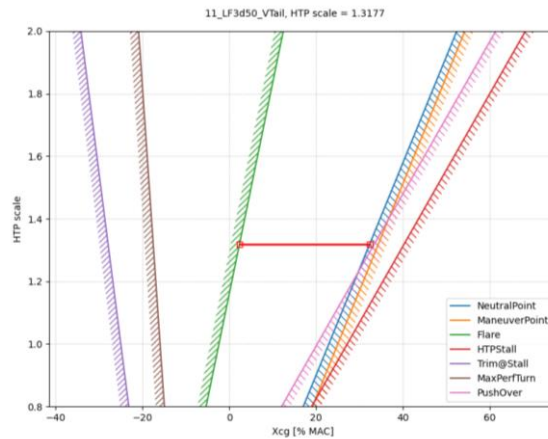


Figure 21 - Longitudinal HQ sizing results

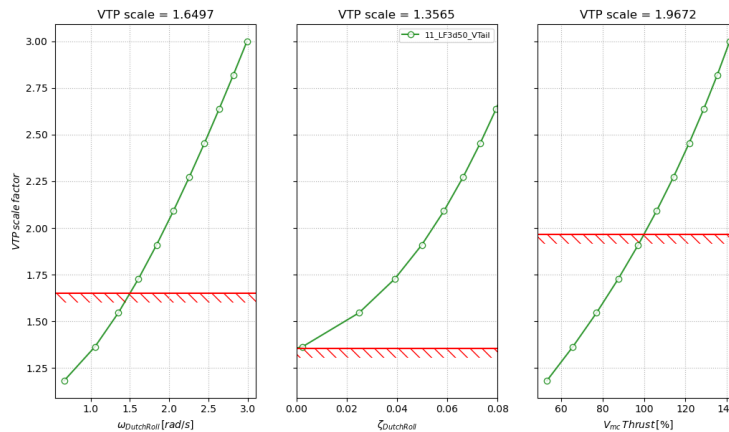


Figure 22 - Lateral/directional HQ sizing results.

#### RANS CFD aero model update

Using the scale factors of the previous paragraph, the aircraft CAD geometry was modified and re-meshed (Figure 23): Table 4 shows a comparison between the initial and recalculated V-tail geometric characteristics. A new set of simulations were launched to provide higher-fidelity estimates of the aerodynamic effects of the updated configuration.

Parameter	Initial V-tail	Resized V-tail
Horizontal Projected area	15.5 m <sup>2</sup>	20.2 m <sup>2</sup>
Vertical Projected area	7.1 m <sup>2</sup>	14.2 m <sup>2</sup>
Total Wetted area	17.0 m <sup>2</sup>	24.7 m <sup>2</sup>
Dihedral	24.5 deg	34.7 deg

Table 4 - Initial VS Resized V-tail geometric parameters

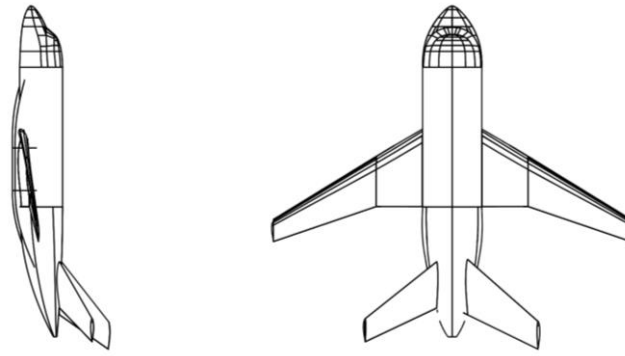


**Figure 23 - Resized (starboard) VS original (port) V-tail**

### Results and Discussion

As part of the selected case study and in accordance with the proposed multi-fidelity sizing procedure, CFD results for the latest configuration were used to calculate aerodynamic increments  $\Delta F_{a_{CFD}}$ , which were then added to the reference (wind tunnel) aerodynamic data. Following this, the HQ-VLM sizing loop was relaunched to update the initial sizing output: The new scale factors were 1.44 and 2.08 for the longitudinal and vertical tail area respectively. The outcome of the process was deemed to be sufficiently close ( $\sim \pm 10\%$ ) to the previous results, satisfying the exit condition of the multi-fidelity sizing loops. Therefore, it was successfully demonstrated that the proposed sizing technique, despite being largely based upon low-fidelity aerodynamic models, managed to address the main limitations of the latter and achieve a considerable increase in accuracy. Of course, in this example, the significant difference in tail size between the reference (wind tunnel) and final configurations would probably require additional wind tunnel testing, however, this was considered to be out of the scope of the intended test application and will not be further analyzed.

## **7. Summary and conclusion**

In this article, the wide fuselage concept was investigated both numerically and experimentally, focusing on the influence of the tail shapes on the aircraft stability.

The RANS CFD computations performed were in good overall agreement with wind tunnel measurements for angles of attack in the range  $\alpha \in [0, 10]^\circ$ , which corresponds to the linear part of the lift coefficient. As far as the pitching moment coefficient is concerned, the trends were correctly reproduced by the numerical simulations, however, the coefficient itself was underestimated for all the configurations considered.

The pitching moment coefficient was the most affected by an increase in fuselage width among aircraft aerodynamic coefficients: The increase of width tends to destabilize the configurations ( $\frac{dC_m}{d\alpha} > 0$ ) due to a forward shift of the aerodynamic center.

From a longitudinal stability standpoint, combined with the associated lift and drag increments, it may be concluded that the T and V tail configurations offer better stabilization in pitch for a given drag penalty than the U tail. If the combined effects on longitudinal and lateral stability are equally considered, the T-tail offers the best overall performance; in the tested configurations this is combined with the highest  $C_{m0}$  value, which should also have a secondary positive effect on trim drag.

In the majority of the tested configurations, an analysis of WT data unveiled unstable characteristics in the longitudinal and directional axis, which, after investigation, was attributed to an inaccurate representation of the stability effects of wide fuselage profiles by the VLM methods used for initial sizing: It was concluded that the latter are sensitive to numerical effects and may differ depending on the method selected for fuselage modelling.

In view of the limitations of the low/medium fidelity aerodynamic prediction methods, a revised tail sizing process was proposed, based on the concept of nested multi-fidelity sizing loops. A test application on the re-sizing of the 3.5m-fuselage V-tail configuration was performed, demonstrating the validity of the proposed methodology.

## 8. Acknowledgement

This study was funded by the European Union under the CleanSky 2 Program through the AIRFRAME ITD NACOR project. The authors would also like to thank Jean Le Gall and Michel Ravachol from Dassault Aviation for their support and suggestions.

## References

- [1] Drela M., “Development of the D8 Transport Configuration”, *29th AIAA Applied Aerodynamics Conference*, 2011
- [2] Wiart et al., “Aeropropulsive Performance Analysis of the NOVA Configurations”, *30th Congress of the International Council of the Aeronautical Sciences*, 2016
- [3] Drela M. and Youngren H., “Athena Vortex Lattice”, *Software Package*, Ver. 3, 2004
- [4] Cambier, L., Heib, S., and Plot, S., “The Onera elsA CFD software: input from research and feedback from industry,” *Mechanics & Industry*, Vol. 14, No. 3, 2013, pp. 159–174.
- [5] Palacios et al., “Stanford University Unstructured (SU2) : An open-Source Integrated Computational Environment for Multi-Physics Simulation and Design”, *51<sup>st</sup> AIAA Aerospace Sciences Meeting and Exhibit*, 2013